

Supplementary materials:

LC-MS/MS method development for the discovery and identification of amphidinols produced by *Amphidinium*

Marvin Wellkamp ¹, Francisco García-Camacho ², Lorena M. Durán-Riveroll ³, Jan Tebben ⁴, Urban Tillmann ⁴, and Bernd Krock ^{4,*}

¹ Alfred-Wegener-Institut für Polar und Meeresforschung, 27570 Bremerhaven, Germany; marvin.wellkamp@web.de

² Chemical Engineering Department, University of Almería, 04120 La Cañada, Almería; fgarcia@ual.es

³ CONACyT-Departamento de Biotecnología Marina, Centro de Investigación Científica y de Educación Superior de Ensenada, 22860 Ensenada, B.C. México; lduran@conacyt.mx

⁴ Section Ecological Chemistry, Alfred Wegener Institute, Helmholtz Centre for Polar and Marine Research, 27570 Bremerhaven, Germany; jan.tebben@awi.de (J.T.); urban.tillmann@awi.de (U.T.)

* Correspondence: Bernd.Krock@awi.de

Figure S1. HRMS-CID-spectrum and fragmentation pattern of LP-D [M+Na]⁺ at *m/z* 1329.7548.

Figure S2. CID-spectrum and fragmentation pattern of AM-22 [M+Na]⁺ at *m/z* 1667.9.

Figure S3. CID-spectrum and fragmentation pattern of LS-A [M+Na]⁺ at *m/z* 1295.8.

Figure S4. CID-spectrum and fragmentation pattern of LP-B/LP-C [M+Na]⁺ at *m/z* 1343.7, here shown on the structure of LP-B.

Figure S5. CID-spectrum and fragmentation pattern of putatively CAR-E [M+Na]⁺ at *m/z* 1421.9.

Figure S6. CID-spectrum and fragmentation pattern of putatively AM-4 [M+Na]⁺ at *m/z* 1323.8.

Figure S7. CID-spectrum and fragmentation pattern of AM-18 [M+Na]⁺ at *m/z* 1381.8.

Figure S8. CID-spectrum and fragmentation pattern of AM-19 [M+Na]⁺ at *m/z* 1483.8.

Figure S9. CID-spectrum and fragmentation pattern of AM-A [M+Na]⁺ at *m/z* 1361.8.

Figure S10. CID-spectrum and fragmentation pattern of AM-A [M+Na]⁺ at *m/z* 1463.8.

Figure S11. CID-spectrum and fragmentation pattern of LP-D [M-H]⁻ at *m/z* 1305.8.

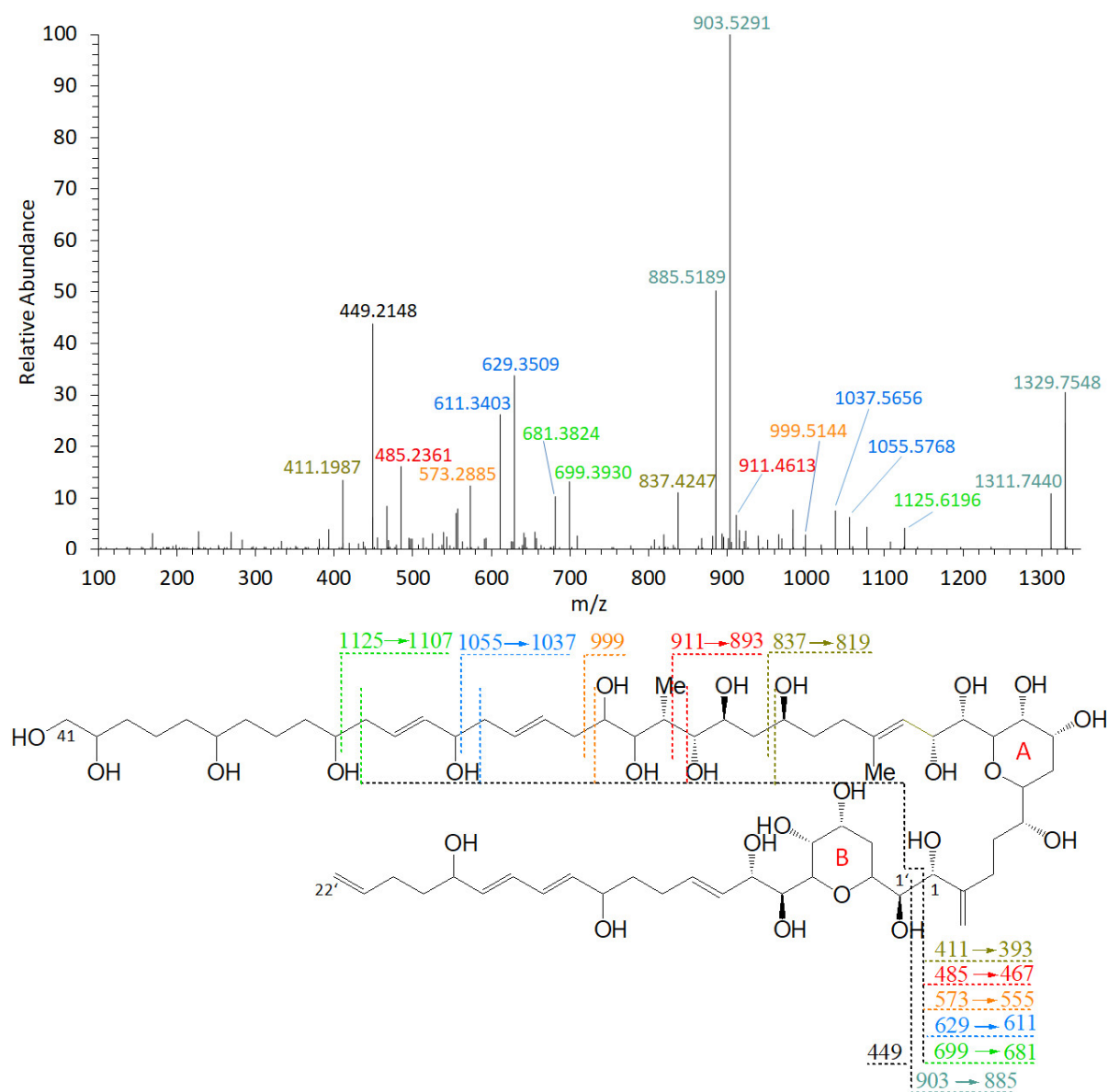


Figure S1. HRMS-CID-spectrum and fragmentation pattern of LP-D $[M+Na]^+$ at m/z 1329.7548.

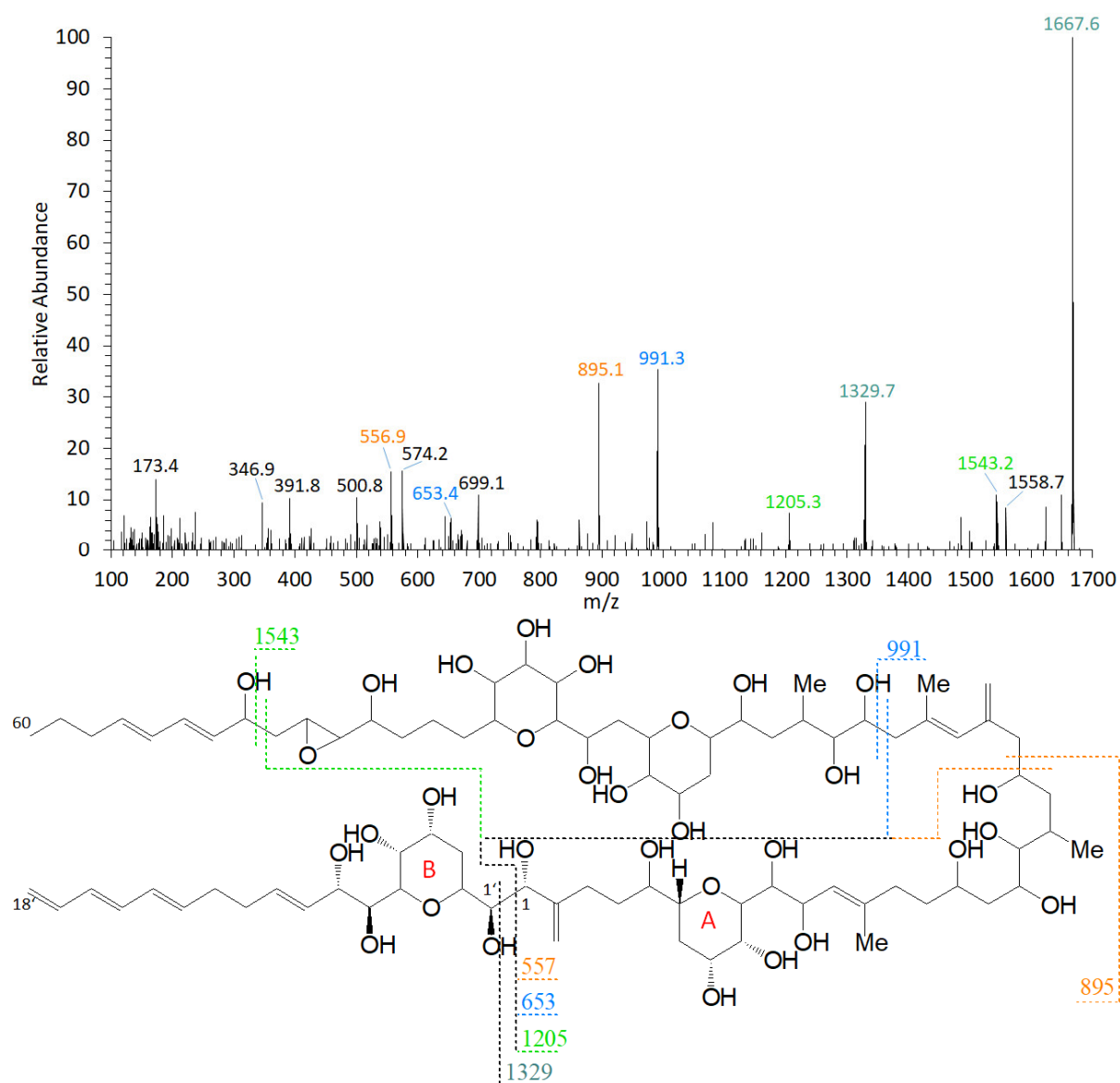


Figure S2. CID-spectrum and fragmentation pattern of AM-22 [M+Na]⁺ at m/z 1667.9.

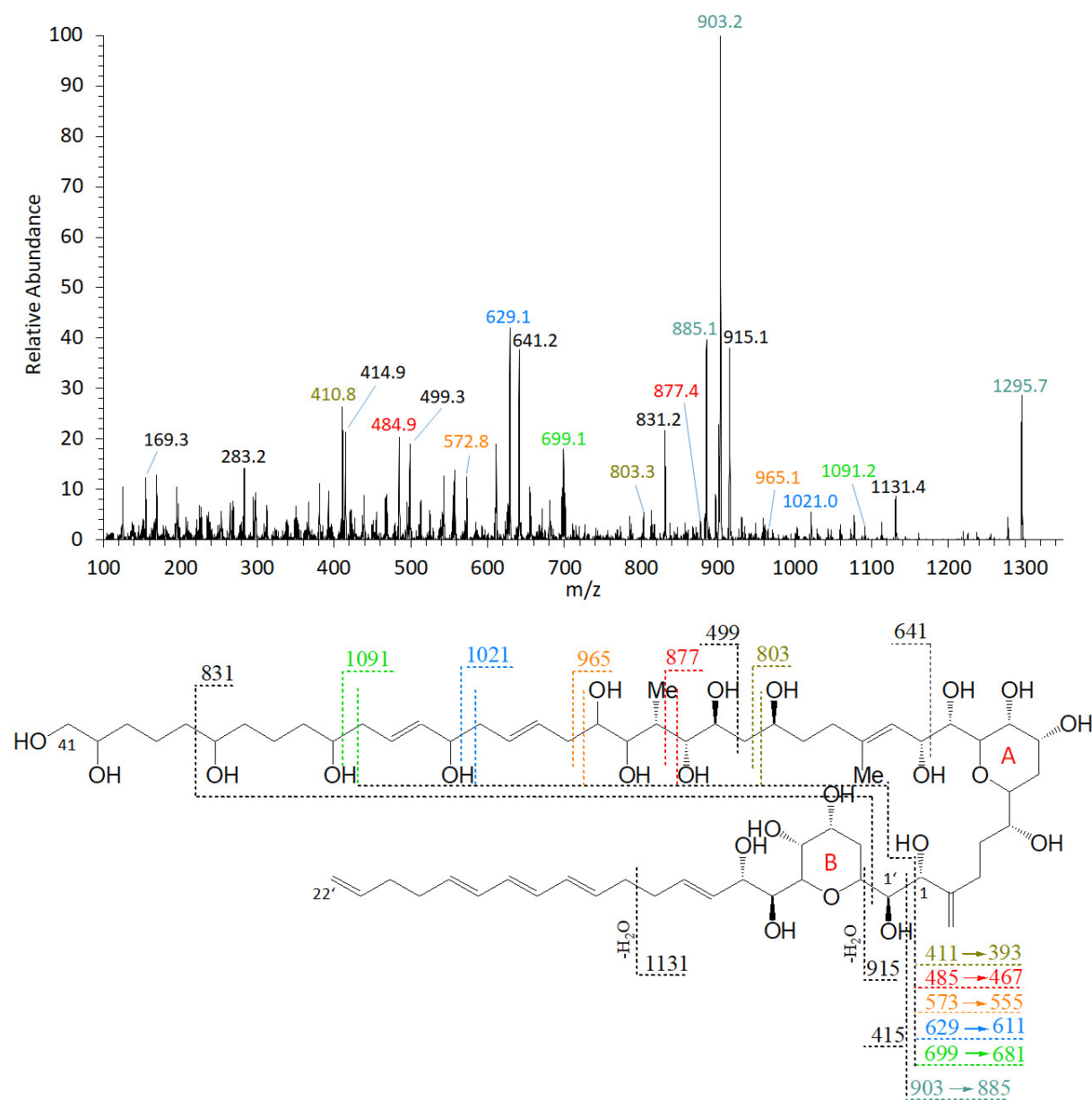


Figure S3. CID-spectrum and fragmentation pattern of LS-A [M+Na]⁺ at m/z 1295.8.

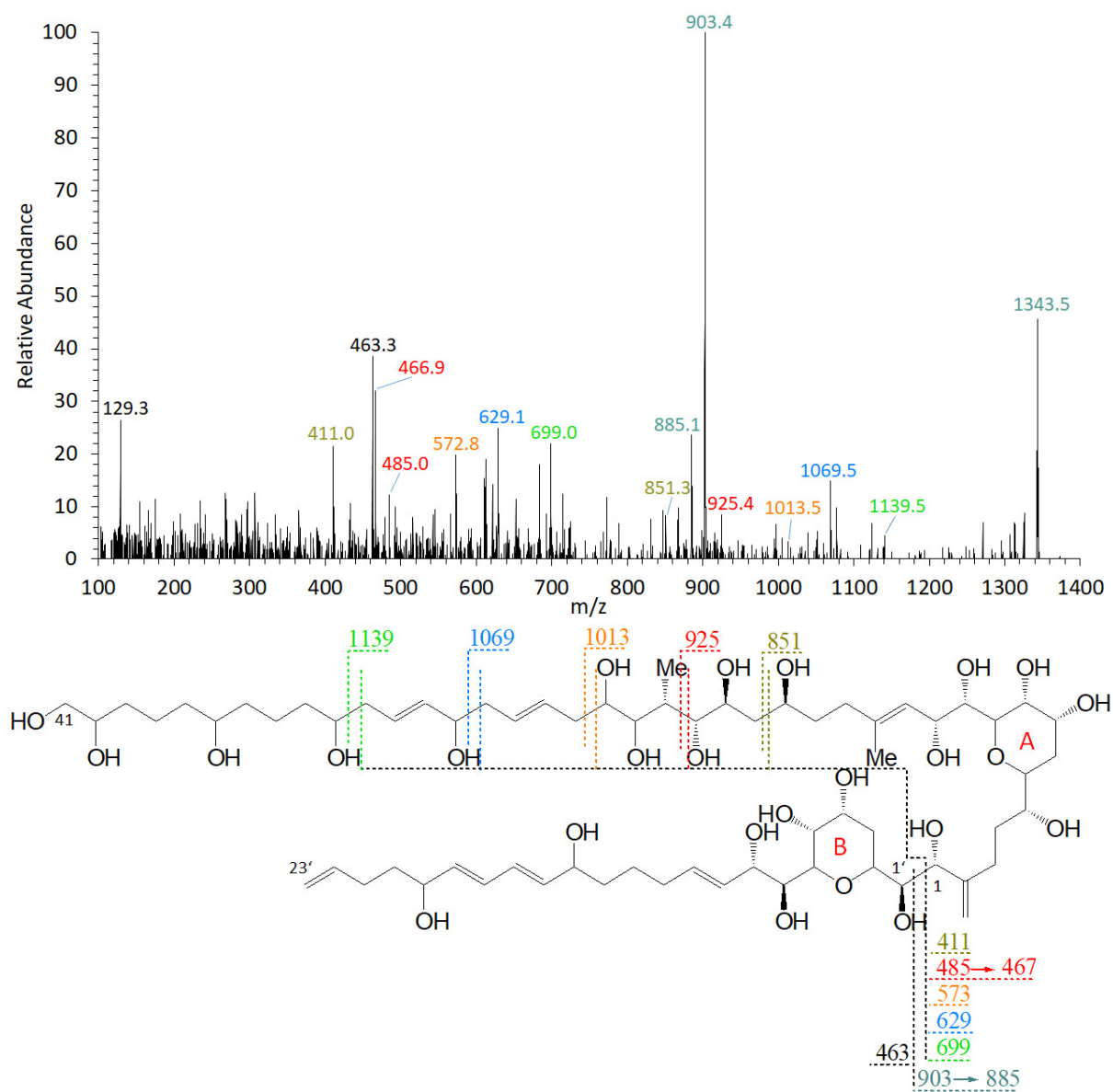


Figure S4. CID-spectrum and fragmentation pattern of LP-B/LP-C $[M+Na]^+$ at m/z 1343.7, here shown on the structure of LP-B.

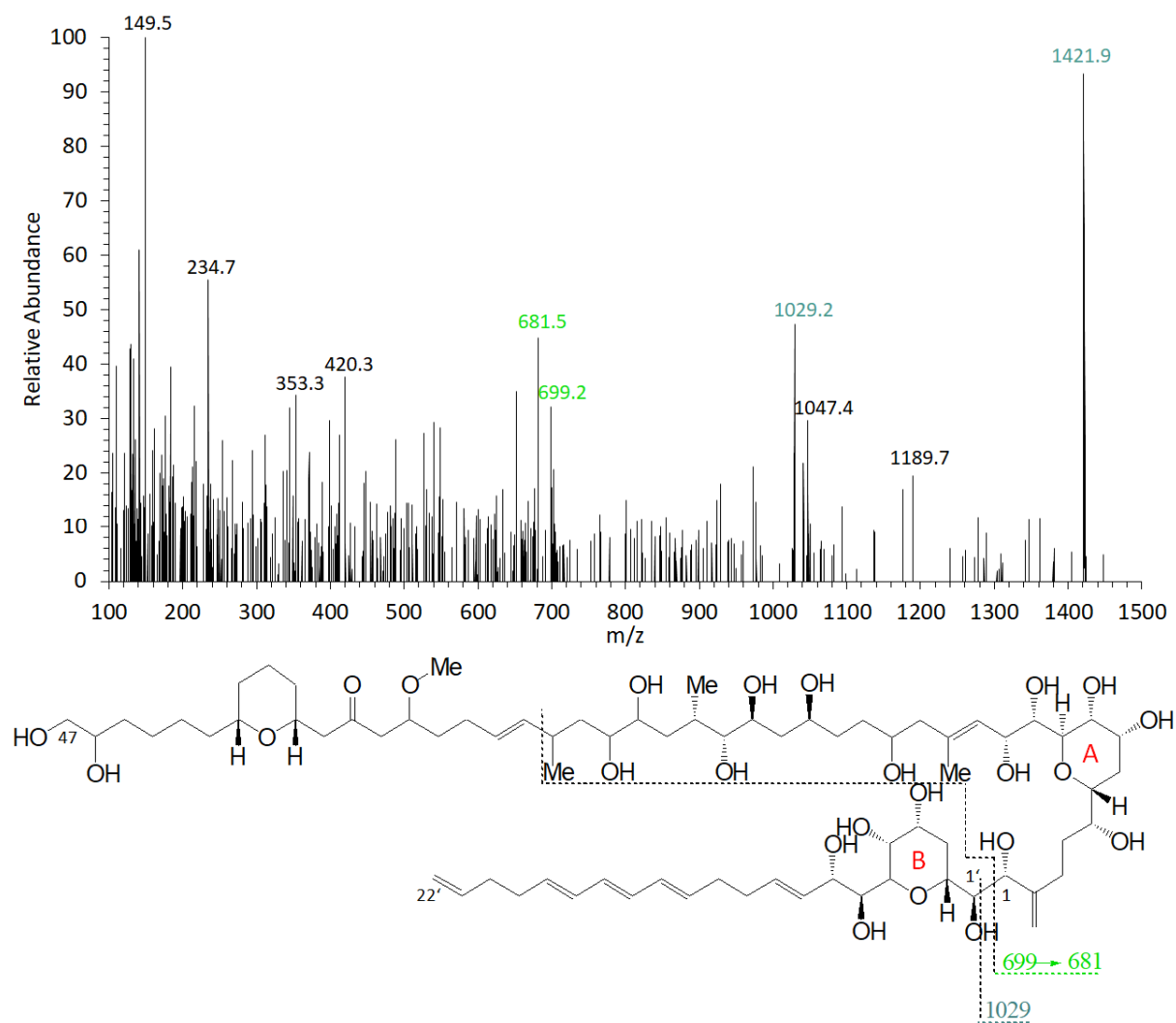


Figure S5. CID-spectrum and fragmentation pattern of putatively CAR-E $[M+Na]^+$ at m/z 1421.9.

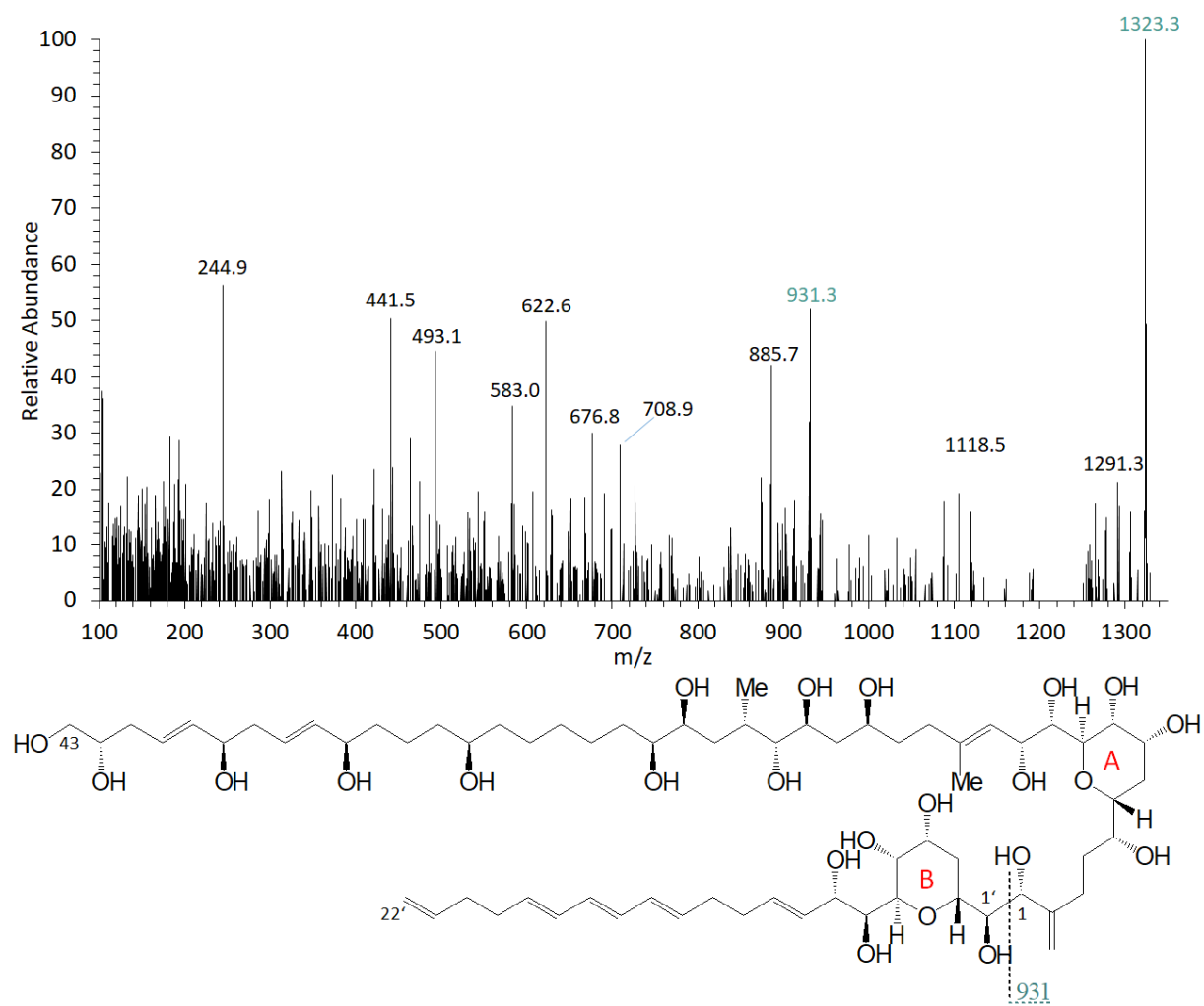


Figure S6. CID-spectrum and fragmentation pattern of putatively AM-4 [M+Na]⁺ at m/z 1323.8.

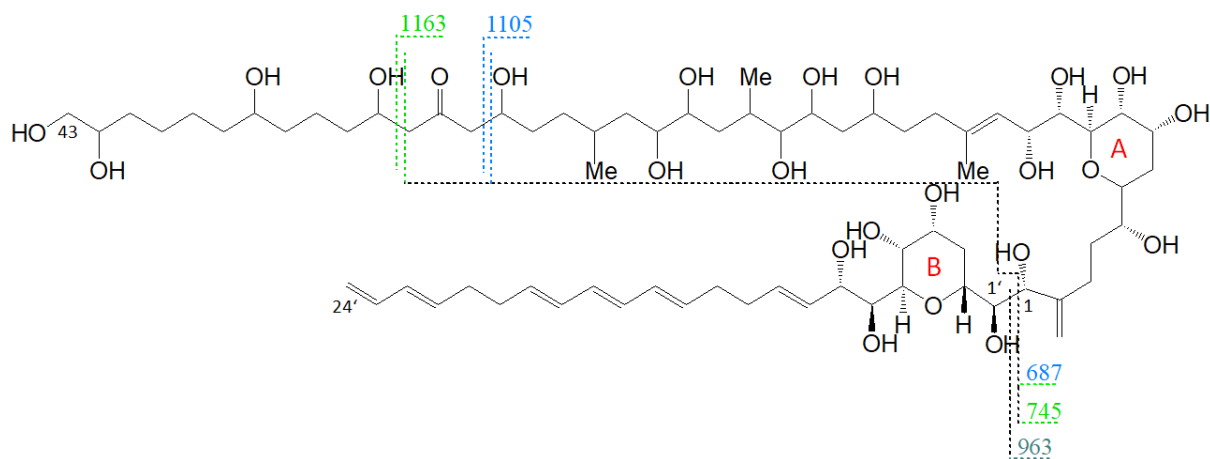
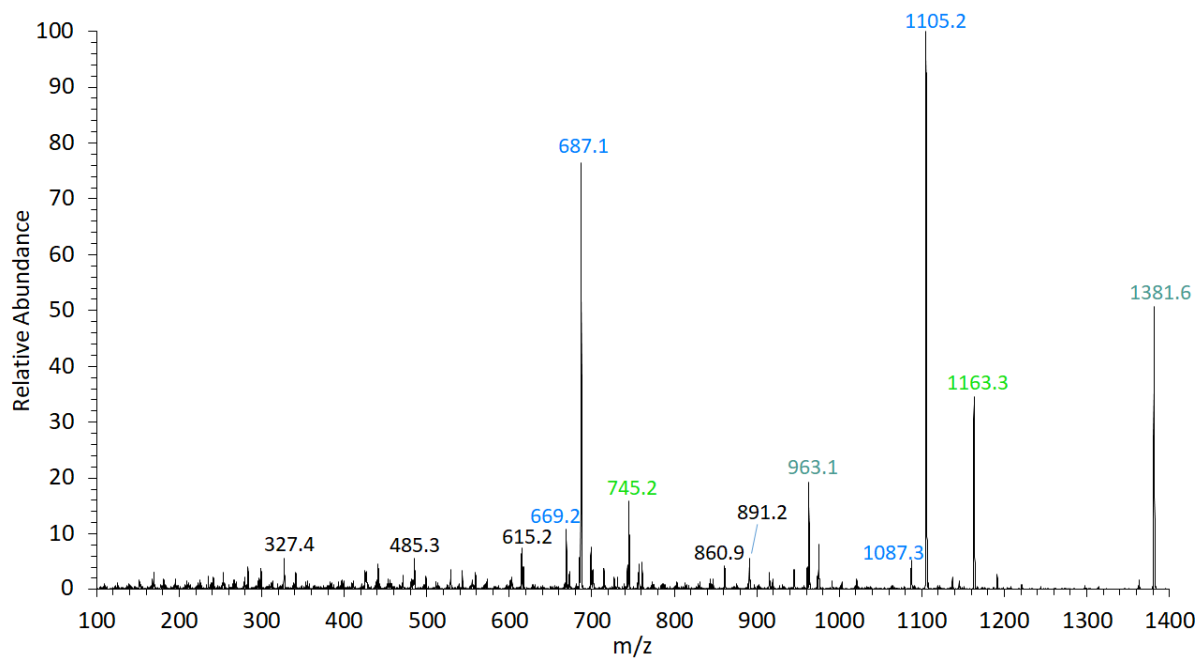
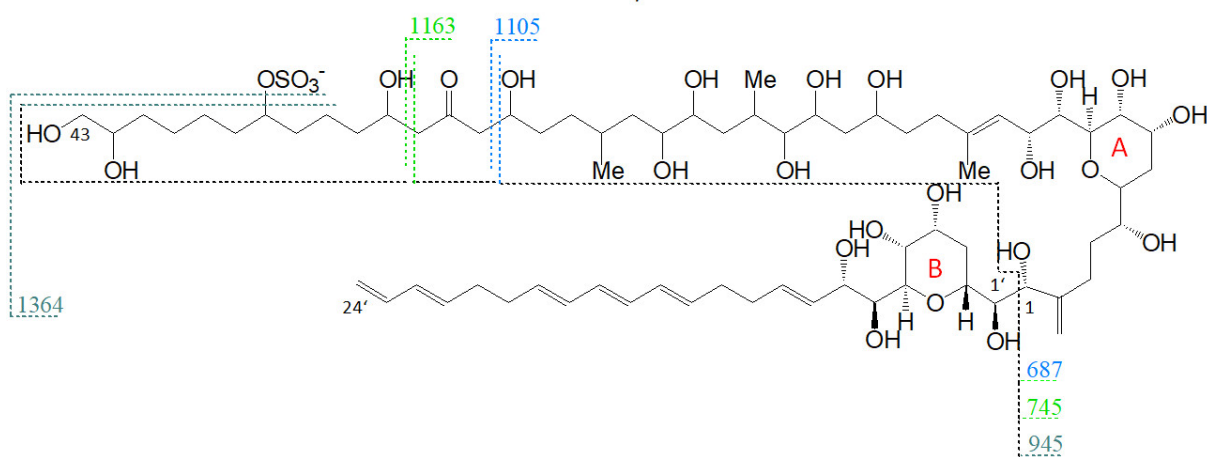
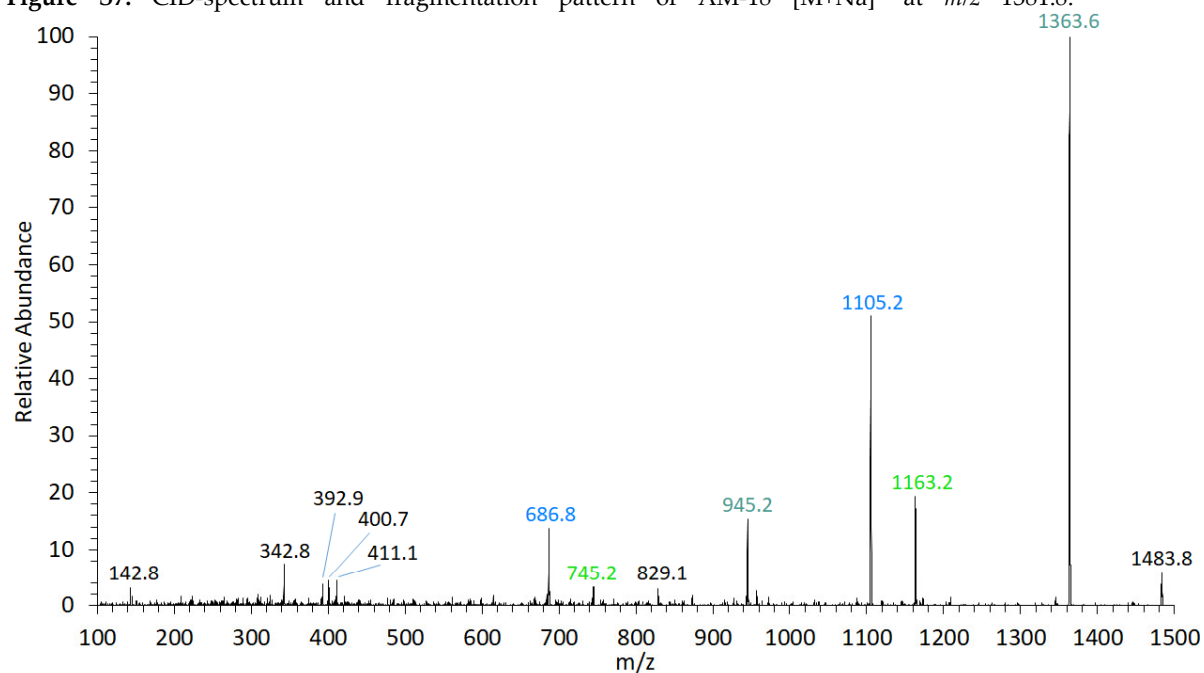


Figure S7. CID-spectrum and fragmentation pattern of AM-18 $[M+Na]^+$ at m/z 1381.8.**Figure S8.** CID-spectrum and fragmentation pattern of AM-19 $[M+Na]^+$ at m/z 1483.8.

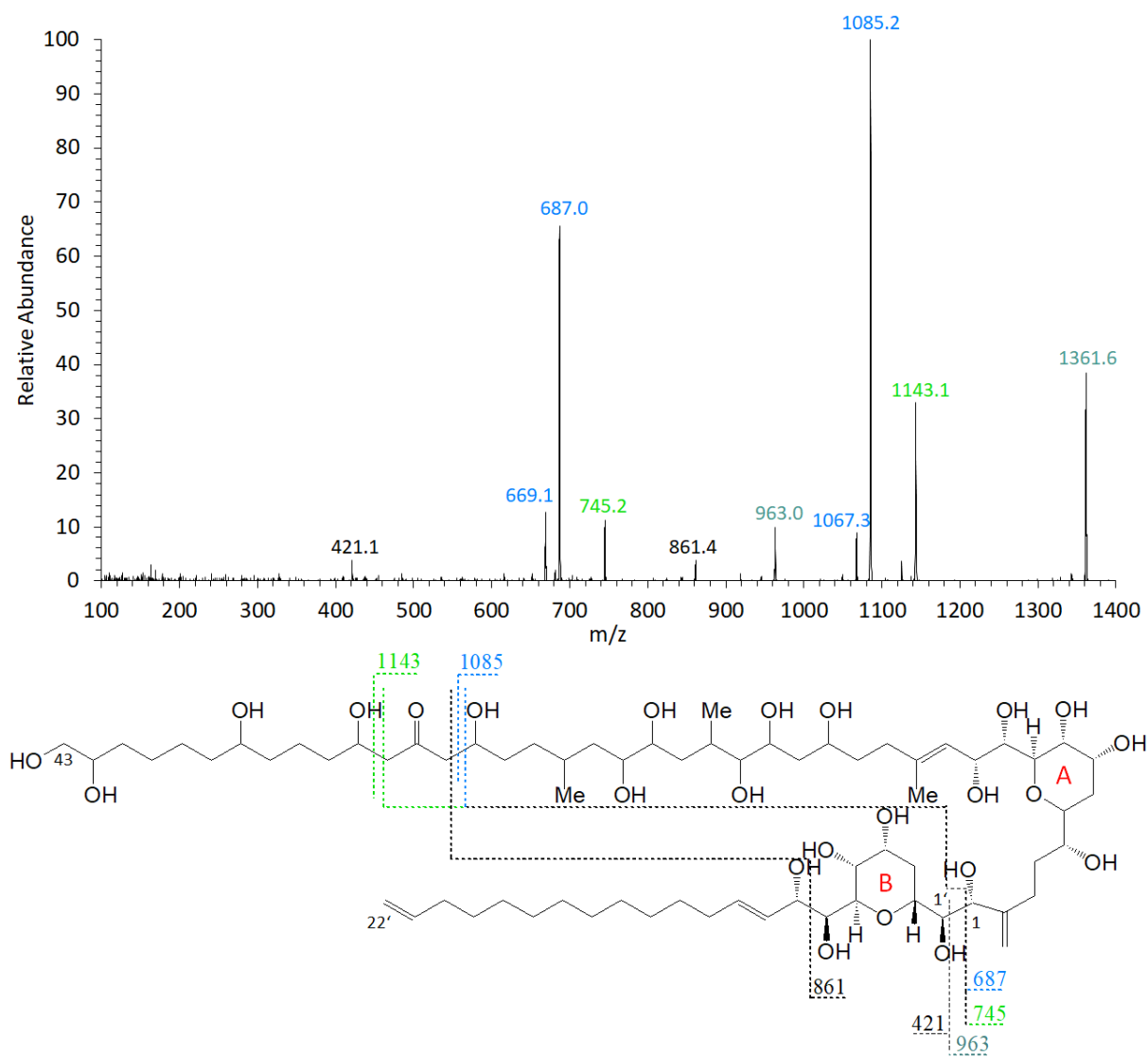


Figure S9. CID-spectrum and fragmentation pattern of AM-A [M+Na]⁺ at m/z 1361.8.

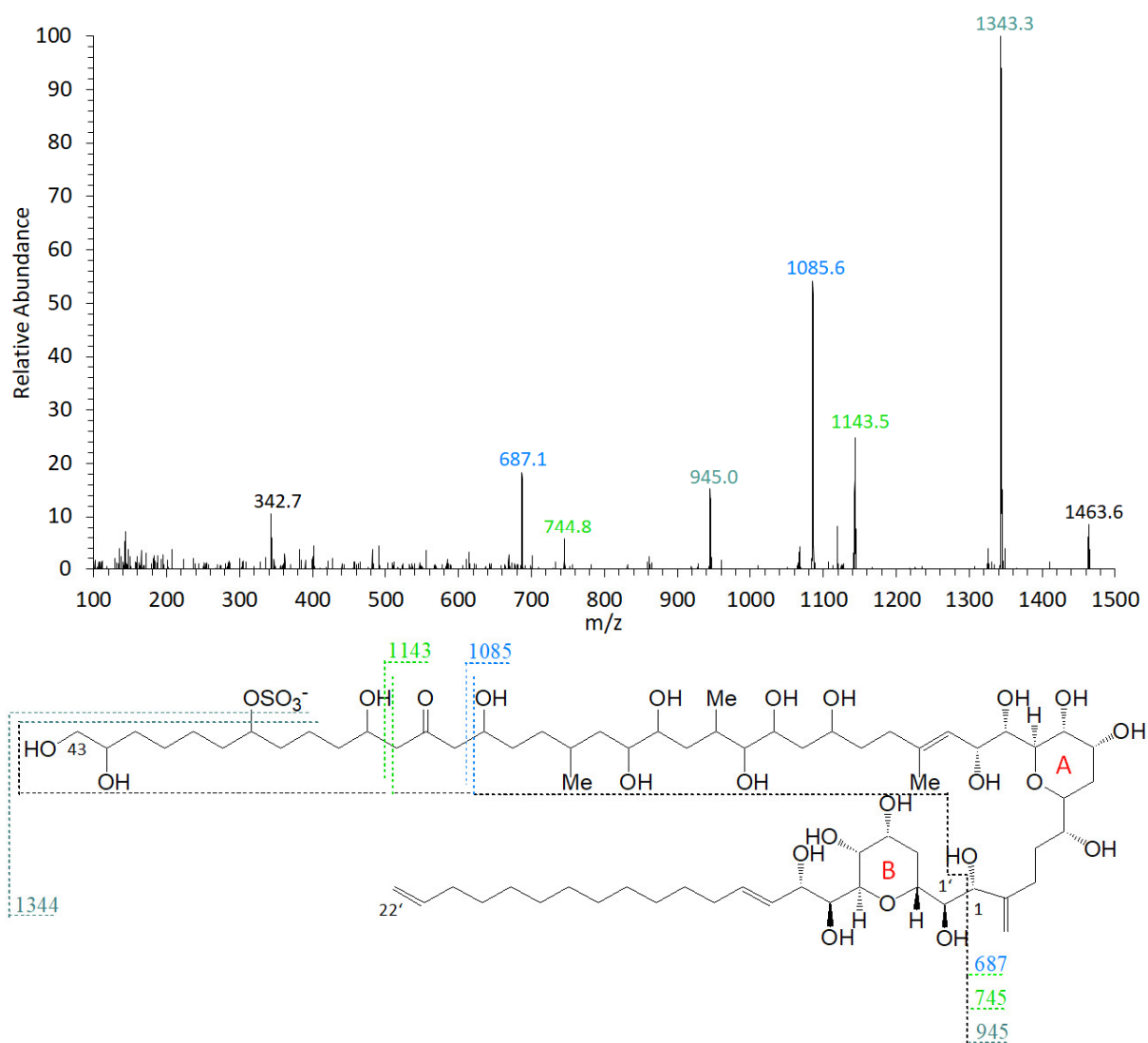


Figure S10. CID-spectrum and fragmentation pattern of AM-A $[M+Na]^+$ at m/z 1463.8.

190630_BK_STD_NEG_05_#213 RT: 2.29 AV: 1 NL: 2.52E6
F: FTMS - p ESI d Full ms2 1305.7654@hcd30.00 [90.0000-1350.0000]

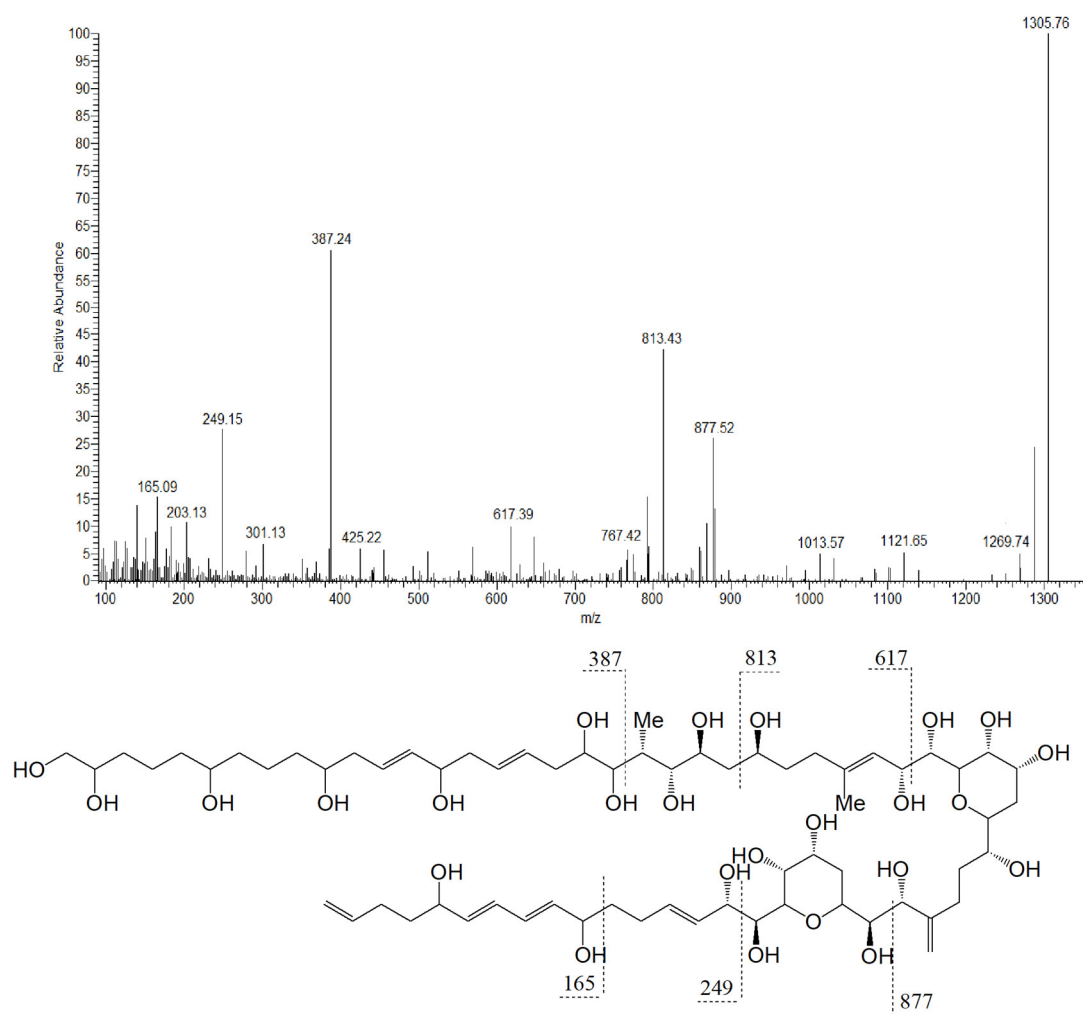


Figure S11. CID-spectrum and fragmentation pattern of LP-D [M-H]⁻ at m/z 1305.8.



© 2020 by the authors. Licensee MDPI, Basel, Switzerland. This article is an open access article distributed under the terms and conditions of the Creative Commons Attribution (CC BY) license (<http://creativecommons.org/licenses/by/4.0/>).